PLIS : An Airborne Polarimetric L-band Interferometric Synthetic Aperture Radar

Doug Gray, Ruiting Yang, Heath Yardley
University of Adelaide Radar Research Centre
EEE School The University of Adelaide
Adelaide, Australia
dgray@eleceng.adelaide.edu.au

Rocco Panciera
Cooperative Research Centre for Spatial Information
Dept. of Infrastructure Engineering:
The University of Melbourne
Melbourne, Australia

Jeffrey Walker
Dept. of Civil Engineering
Monash University
Melbourne, Australia

Jorg Hacker, Andrew McGrath
Airborne Research Australia
School of the Environment, Flinders University
Adelaide, Australia

Bevan Bates
DSTO Edinburgh/University of Adelaide
Adelaide, Australia

Nick Stacy
DSTO Edinburgh
Adelaide, Australia

Abstract—**PLIS is an airborne synthetic aperture radar designed to be used in conjunction with a passive radiometer to collect microwave data at L-band for the remote sensing of soil moisture. The objective is to collect data to carry out a pre-deployment validation of algorithms for the NASA Soil Moisture Active Passive (SMAP) satellite. Key features of the PLIS radar are described. The ground swath of PLIS is such that the incidence angle ranges from 15 degrees from nadir on the near side of the swath to 45 degrees on the far side, resulting in an almost 3:1 variation in ground range resolution across the swath. Initial investigations into the impact of this on the statistics of backscattered data are presented.**

Keywords- Synthetic Aperture Radar; Soil moisture; L-band radar, SMAP, Polarimetric Radar

I. INTRODUCTION

Soil moisture, through evapotranspiration, plays a major role in the evolution of weather and climate and obtaining global measurements of soil moisture levels in the top 5cm of the earth's surface at revisit rates on the order of 3 days will provide valuable input into both local weather and global climate models. NASA plans to deploy the SMAP satellite with both an active L-band scatterometer and a passive L-band radiometer to achieve this. SMAP will simultaneously collect active and passive microwave data soil moisture data from both sensors that can be later fused to achieve global soil moisture data at a spatial resolution of 3-10km, significantly improving on the 40km resolution achieved by a radiometer alone. SMAP is a sun-synchronous low-earth orbit satellite collecting data across a wide swath of ~1000km using conical scanning at a constant incidence angle of 40 degrees and is currently scheduled for launch around 2015 [1].

In order to allow pre-deployment validation of the SMAP concepts and algorithms Australia has acquired an airborne L-band radiometer (PLMR : Passive L-band Multibeam Radiometer) and an L-band radar (PLIS : Polarimetric L-Band Interferometric SAR). PLIS is a fully polarimetric airborne interferometric synthetic aperture digital radar, delivered in early to mid 2010 and since then has been used in a number of experimental airborne trials as well as two major field campaigns, SMAPEx-1,2. A characteristic of the PLIS antennas is that the incidence angle, measured from nadir, varies from 15 degrees on the near side of the ground swath to 45 degrees on the far side, resulting in an almost 3:1 variation in ground range resolution across the swath. After a short description of the PLIS radar in Section II, initial investigations into the impact of this on the statistics of the backscattered data are presented in Sections III and IV.

II. PLIS DESCRIPTION

PLIS is a polarimetric airborne interferometric synthetic aperture digital radar that uses microstrip antennas to radiate and receive. It has been designed to be mounted either underneath or on the wing of a light aircraft, see Figure 1, and typically operates at heights varying from ~300m to ~3000m with the aircraft typically flying at speeds of 40 to 120 m/s. It radiates pulsed LFM chirps at a carrier frequency of 1.26GHz with bandwidths up to 30MHz in either H or V polarisation modes at typical pulse repetition frequencies of around 2-8 kHz. A dual channel receiver allows it to simultaneously receive and sample both H and V polarizations. PLIS illuminates ground swaths either side of the aircraft and has secondary antennas, used for interferometry, that can be mounted on the other wing of a light aircraft, ~9 metres for the configuration shown in Figure 1. Key features of the various components are described in the following sections.

The PLIS radar was developed and purchased using funds from the Australian Research Council's *LIEF* funding scheme (project number LE0882509)

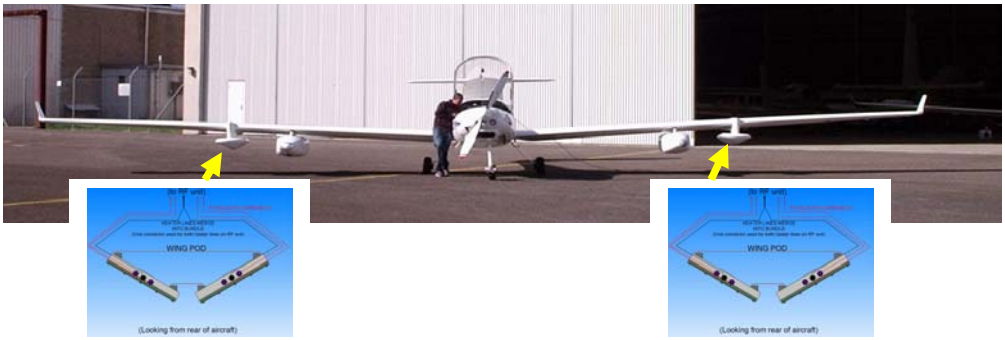

Figure 1. PLIS main and auxiliary antennas

A. *Waveform Generation and RF Circuitry*

The output from a direct digital synthesizer, DDS, either unmodulated or linear FMCW pulsed waveforms, are single stage upconverted to RF by mixing with the output from a 1170MHz phase locked oscillator, The pulse width can be varied from 100ns to 10μs and the bandwidth can varied up to 30MHz with the system normally transmitting a 30MHz bandwidth chirp. The pulse repetition frequency, PRF, can be increased to 20kHz subject to the duty cycle not exceeding 4%. A cavity filter of 25MHz bandwidth prior to a 30W peak solid state power amplifier band-limits the transmitted signal to minimize transmitted power in the nearby GPS band.

The transmit signal can be fed via an attenuator directly to the H and V ports of the down-converters prior to the digital receiver thus providing both a real time monitoring capability and an internal calibration signal.

B. *Transmit and Receive Antennas*

After various filters, switches and circulators the RF signal is fed into a two port network that switches the transmit signal between the right and left antenna of the main antenna each orientated with their broadside direction at 45 degrees to nadir as illustrated in Figure 1. An additional two port network switches the transmit antenna between H and V polarizations. PLIS can be configured by a GUI to radiate all four possible interleaved transmission sequences at the expense of a concomitant reduction in the effective pulse repetition frequency.

Each antenna consists of a 2×2 grid of patch antennas and the aperture of the grid is ~20cm giving a measured one-way 3dB beamwidth of 51 degrees and a two-way beamwidth of ~26 degrees. The measured gain of each antenna is ~9dBi and the cross-polarisation isolation was measured to be in excess of 30dB. The system noise figure is ~5.2dB

C. *Digital Receiver and Data Recording*

After single stage down conversion, data from the H and V receive channels is fed into a dual channel digital receiver, the Mercury Echotek ECV4-2-2R130, where two 16 bit digitisers sample the data at a rate of 120Msamples/s. An onboard FPGA implements digital down-conversion to baseband and decimation filtering. A Spectracom TSync-PCIe board locks onto GPS signals and provides an accurate timestamp for data acquisition.

Data from each pulse is recorded for a user-defined number of range bins and the record data rate is dependent on the various polarisation/antenna options chosen for transmission and receive.

III. GROUND SWATH ISSUES

The orientation of the antennas and the relatively large vertical beamwidth of ~51 degrees for each transmit and receive antenna results in a steep incidence angle, relative to nadir, varying from 15 degrees to 45 degrees across the swath. The resulting varying ground range resolution implies a varying sensitivity across the swath which is investigated in this section.

A. *Ground Range Resolution*

At a 20MHz transmit bandwidth the slant range resolution is 7.5m however at the far edge of the beam, i.e., at 45 degrees off nadir, the ground range resolution for a 20MHz signal will be ~11m, whilst at the beam centre it will be ~15m and at the near edge of the beam, i.e., at 15 degrees off nadir, the ground range resolution will be ~29m, as illustrated in Figure 2.

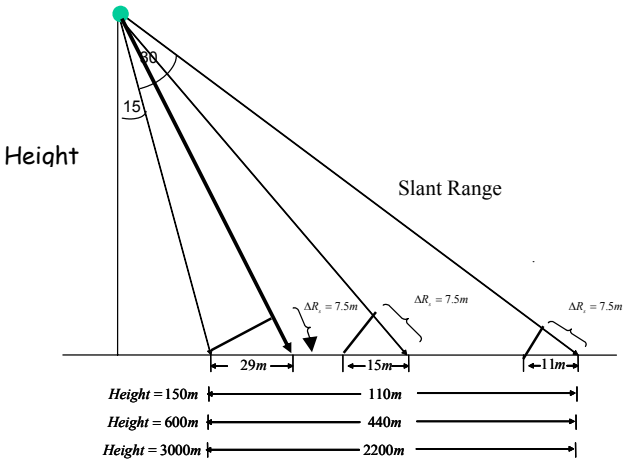

Figure 2. Variability of PLIS ground resolution across a swath

B. *System Sensitivity*

The first impact of this will be a variation of system sensitivity across the swath. For surface scattering the minimum noise equivalent normalized radar cross-section is defined as when the received backscatter power equals the thermal noise power and is given by

$$(NRCS)_{\min} = \frac{256.\pi^3.R^3.k.T.B.F.\sin\phi.v_y}{PRF.P_t.G^2.\lambda^3.c.\tau}$$

where F is the system noise figure, ϕ is the beam angle off nadir, v_y the along track aircraft speed, P_t the transmit power, G the antenna gain and τ the pulse width. A typical example of this is plotted in Figure 3 implying reduced return signal power for range cells covering the outer part of the swath.

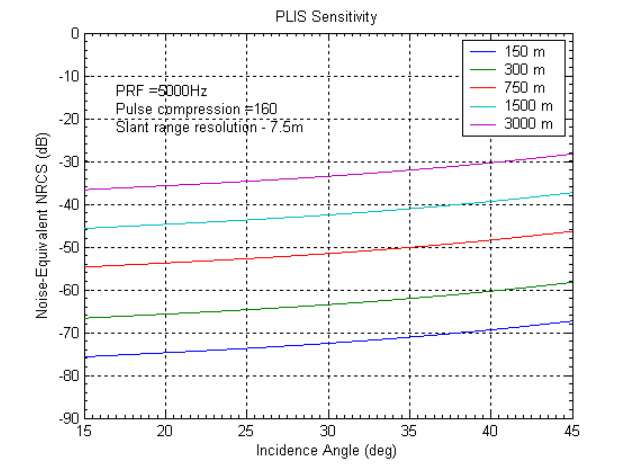

Figure 3. PLIS sensitivity versus angle and height

Note that the shape of the angular/across swath variations are independent of the height of the aircraft and typically indicate an ~8dB reduction in backscatter strength across the swath.

IV. Experimental Measurments

To measure the variation in back-scatter strength across the PLIS swath, data from experiments where PLIS was flown over a relatively homogeneous and flat area of mangroves at Dry Creek near Adelaide, South Australia, was analysed.

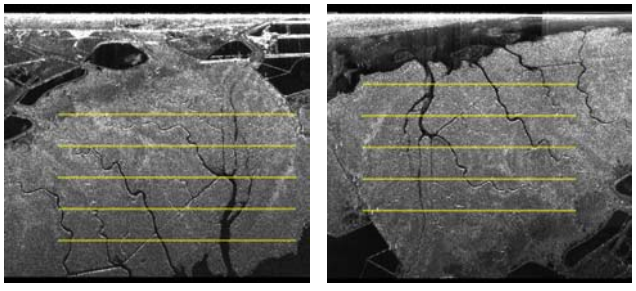

(a) P1 (b) P4

Figure 4. PLIS image showing the range slices used to estimate histograms – the two plots of the same area are from opposite directions and at different ranges

Figure 4 shows the PLIS image of one such area with the yellow lines indicating five particular range bins selected for analysis. Note range runs down the page and cross-range across the page. At each selected range, a total of 400 cross-range bins were used to estimate the histogram of return powers for the various transmit/receive combinations VV, VH, HV and HH. The histograms corresponding to Figure 4(a) are shown in Figure 5 for the HH mode and in Figure 6 for the VV mode.

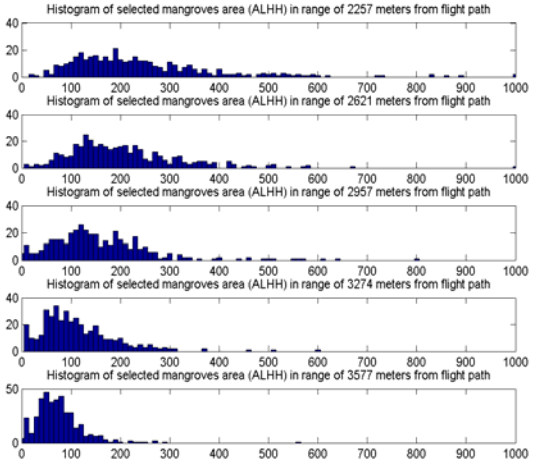

Figure 5. Backscatter powers histograms HH mode

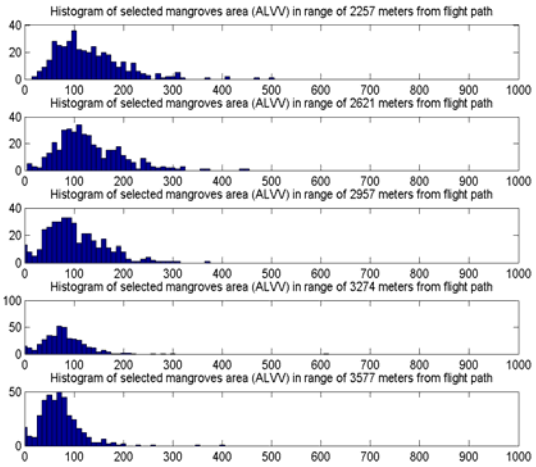

Figure 6. Backscatter powers histograms VV mode

Both examples indicate that the backscattered signal strength decreases with range but not to the extent indicated in Figure 3. (Note that as a full calibration of the system has not yet been achieved absolute units for the back-scatter strengths have not been presented – this is not a problem here as this investigation is concerned with relative variations in power across the swath width.)

To quantify this result thresholded backscattered powers averaged over 400 azimuthal bins and at slant range intervals of 3.75m covering the rectangular area defined by the lines of Figure 4(a) and 4(b) is plotted in Figure 7 for both HH and VV.

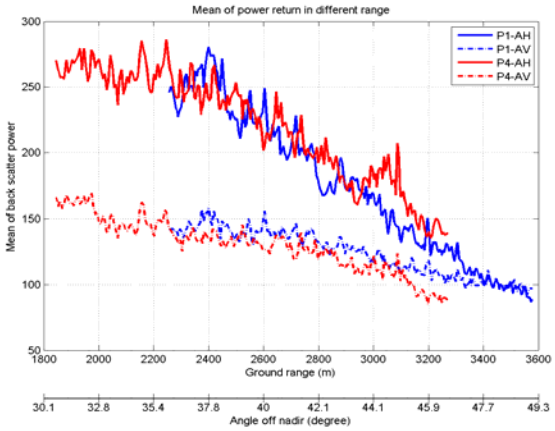

Figure 7. Range variation of mean and variance of HH and VV returns

The results indicate little change in the HH and VV back-scatter powers over ground ranges varying from ~1800m to ~2200m or alternatively incidence angles varying from 30 to 35 degrees. This result is not consistent with Figure 3 which indicates a 2dB reduction in backscatter power. From ~2200m to ~3600m, or equivalently incidence angles from 35 to 50 degrees, the reduction is ~4 dB for the HH mode and ~1.8dB for the VV mode. Over this range Figure 3 predicts a reduction of ~6dB so again the experimental results are not in close agreement with theory. It is worth mentioning that in areas where the ranges overlap the measured powers from opposite directions are in reasonable agreement implying possible angular invariance of the results.

Two other areas, as illustrated in Figure 8 were considered : both areas had a number of range bins at the same range.

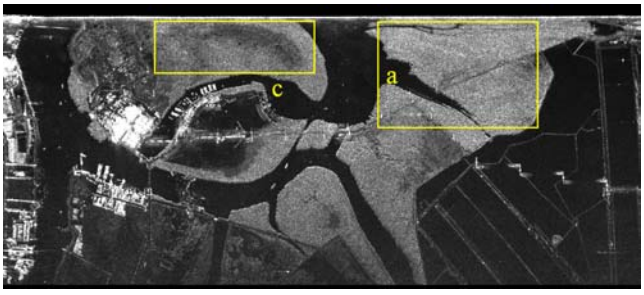

Figure 8. HV image of two further sites

The average thresholded power across 300 azimuth bins for both areas are plotted in Figure 9 with the results showing some consistency between the two sites for VV mode but not the HH mode. Similarly to the results presented in Figure 7 there is a difference between the angular variation of the HH and VV returns although the difference between the dB angular variations is not as great.

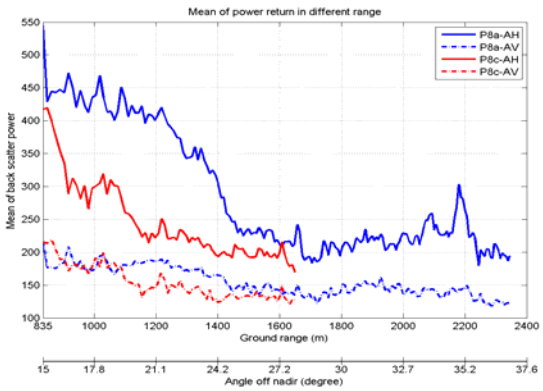

Figure 9. HH and VV return strength versus range

Figure 10 plots the mean power of the HH and VV backscattered returns from an area of sea surface in gulf waters - the sea conditions were calm and the wind speed was low.

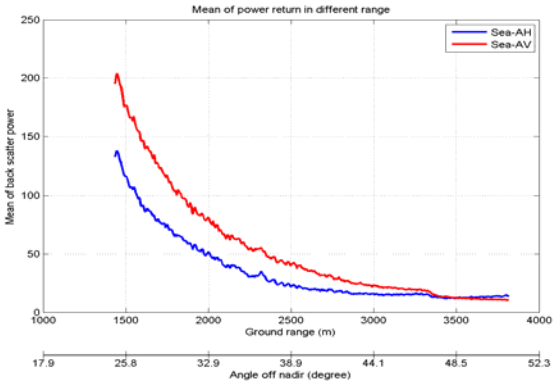

Figure 10. HH and VV sea surface returns

Although weak, the sea surface back-scatter returns show a well defined range dependency with a clear difference between the HH and VV results.

V. SUMMARY

The PLIS airborne synthetic aperture radar has been described and experimental results measuring the relative variation of the strength of the backscatter signal across the swath width have been presented. The results show only qualitative agreement with theoretical predictions based on a model where the normalized radar cross-section is independent of angle. Future work to refine this model to provide a better fit to the experimental data is required. Further work is also required to repeat this analysis using calibrated data and to investigate any possible biases due to leakage from the strong altitude return.

REFERENCES

[1] D Entekhabi, EG Njoku, PE O'Neill et al., "The Soil Moisture Active Passive (SMAP) Mission" Proc IEEE, pp. 704 - 716, May 2010.